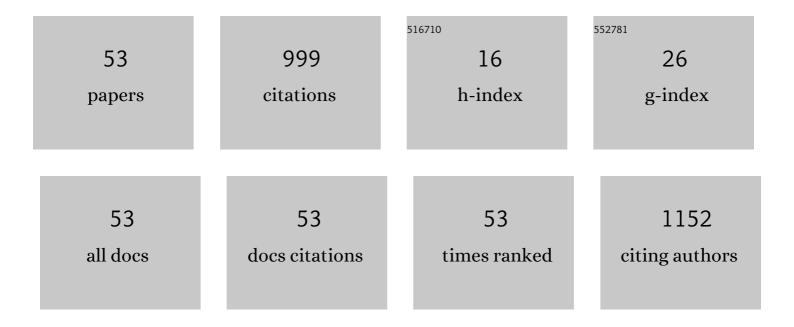
## **Cristian Rossi**

List of Publications by Year in descending order

Source: https://exaly.com/author-pdf/3964749/publications.pdf

Version: 2024-02-01



#	Article	IF	CITATIONS
1	TanDEM-X calibrated Raw DEM generation. ISPRS Journal of Photogrammetry and Remote Sensing, 2012, 73, 12-20.	11.1	138
2	Quality Assessment of Surface Current Fields From TerraSAR-X and TanDEM-X Along-Track Interferometry and Doppler Centroid Analysis. IEEE Transactions on Geoscience and Remote Sensing, 2014, 52, 2759-2772.	6.3	87
3	Paddy-Rice Monitoring Using TanDEM-X. IEEE Transactions on Geoscience and Remote Sensing, 2015, 53, 900-910.	6.3	73
4	Interferometric processing of TanDEM-X data. , 2011, , .		71
5	Remote monitoring to predict bridge scour failure using Interferometric Synthetic Aperture Radar (InSAR) stacking techniques. International Journal of Applied Earth Observation and Geoinformation, 2018, 73, 463-470.	2.8	63
6	Towards Sentinel-1 SAR Analysis-Ready Data: A Best Practices Assessment on Preparing Backscatter Data for the Cube. Data, 2019, 4, 93.	2.3	56
7	Urban DEM generation, analysis and enhancements using TanDEM-X. ISPRS Journal of Photogrammetry and Remote Sensing, 2013, 85, 120-131.	11.1	41
8	Temporal monitoring of subglacial volcanoes with TanDEM-X — Application to the 2014–2015 eruption within the Bárðarbunga volcanic system, Iceland. Remote Sensing of Environment, 2016, 181, 186-197.	11.0	39
9	Combined InSAR and Terrestrial Structural Monitoring of Bridges. IEEE Transactions on Geoscience and Remote Sensing, 2020, 58, 7141-7153.	6.3	39
10	Polarization Impact in TanDEM-X Data Over Vertical-Oriented Vegetation: The Paddy-Rice Case Study. IEEE Geoscience and Remote Sensing Letters, 2015, 12, 1501-1505.	3.1	37
11	Early warning system for the detection of unexpected bridge displacements from radar satellite data. Journal of Civil Structural Health Monitoring, 2021, 11, 189-204.	3.9	29
12	A Nonlocal InSAR Filter for High-Resolution DEM Generation From TanDEM-X Interferograms. IEEE Transactions on Geoscience and Remote Sensing, 2018, 56, 6469-6483.	6.3	28
13	Interferometric processing and products of the TanDEM-X mission. , 2012, , .		25
14	Geomorphometric analysis of the 2014–2015 Bárðarbunga volcanic eruption, Iceland. Remote Sensing of Environment, 2018, 204, 244-259.	11.0	25
15	The worsening impacts of land reclamation assessed with Sentinel-1: The Rize (Turkey) test case. International Journal of Applied Earth Observation and Geoinformation, 2019, 74, 57-64.	2.8	22
16	Framework for Fusion of Ascending and Descending Pass TanDEM-X Raw DEMs. IEEE Journal of Selected Topics in Applied Earth Observations and Remote Sensing, 2015, 8, 3347-3355.	4.9	21
17	Integration of SAR Data Into Monitoring of the 2014–2015 Holuhraun Eruption, Iceland: Contribution of the Icelandic Volcanoes Supersite and the FutureVolc Projects. Frontiers in Earth Science, 2018, 6, .	1.8	21

18 Fast document-at-a-time query processing using two-tier indexes. , 2013, , .

**CRISTIAN ROSSI** 

#	Article	IF	CITATIONS
19	High-Resolution InSAR Building Layovers Detection and Exploitation. IEEE Transactions on Geoscience and Remote Sensing, 2015, 53, 6457-6468.	6.3	18
20	Fast top-k preserving query processing using two-tier indexes. Information Processing and Management, 2016, 52, 855-872.	8.6	16
21	Waves: a fast multi-tier top-k query processing algorithm. Information Retrieval, 2017, 20, 292-316.	2.0	13
22	Processing of bistatic TanDEM-X data. , 2010, , .		11
23	Single-Pass Tomography With Alternating Bistatic TanDEM-X Data. IEEE Geoscience and Remote Sensing Letters, 2015, 12, 409-413.	3.1	11
24	SmallSats: a new technological frontier in ecology and conservation?. Remote Sensing in Ecology and Conservation, 2022, 8, 139-150.	4.3	11
25	Surface current retrieval from TerraSAR-X data using Doppler measurements. , 2010, , .		10
26	Decadal Earth topography dynamics measured with TanDEM-X and SRTM. , 2012, , .		9
27	Fusion of ascending and descending pass raw TanDEM-X DEM. , 2014, , .		8
28	Monitoring deformations of Istanbul metro line stations through Sentinel-1 and levelling observations. Environmental Earth Sciences, 2021, 80, 1.	2.7	6
29	Framework for Remote Sensing and Modelling of Lithium-Brine Deposit Formation. Remote Sensing, 2022, 14, 1383.	4.0	6
30	Interferometric processing algorithms of TanDEM-X data. , 2010, , .		5
31	A polarimetric temporal scene parameter and its application to change detection. , 2011, , .		4
32	<scp>LePrEF</scp> : Learn to precompute evidence fusion for efficient query evaluation. Journal of the Association for Information Science and Technology, 2012, 63, 1383-1397.	2.6	4
33	TanDEM-X for mass balance of glaciers and subglacial volcanic activities. , 2015, , .		4
34	Development of a subglacial lake monitored with radio-echo sounding: case study from the eastern Skaftá cauldron in the Vatnajökull ice cap, Iceland. Cryosphere, 2021, 15, 3731-3749.	3.9	4
35	Comparison of in situ and interferometric synthetic aperture radar monitoring to assess bridge thermal expansion. Proceedings of the Institution of Civil Engineers - Smart Infrastructure and Construction, 2022, 175, 73-91.	1.7	4
36	Phenological growth stages of paddy rice according to the BBCH scale and SAR images. , 2014, , .		3

**CRISTIAN ROSSI** 

#	Article	IF	CITATIONS
37	Nonlocal InSAR filtering for high resolution DEM generation from TanDEM-X interferograms. , 2017, , .		3
38	Testing the Interoperability of Sentinel 1 Analysis Ready Data Over the United Kingdom. , 2018, , .		3
39	Understanding Insar Measurement Through Comparison With Traditional Structural Monitoring - Waterloo Bridge, London. , 2019, , .		3
40	NRT-Monitoring am Vulkanausbruch Eyjafjallajokull (Island) mit TerraSAR-X. Photogrammetrie, Fernerkundung, Geoinformation, 2010, 2010, 339-354.	1.2	2
41	First urban TanDEM-X RawDEMs analysis. , 2011, , .		2
42	Generation of rice crops temporal change maps with differential TanDEM-x interferometry. , 2014, , .		2
43	An Earth Observation Framework for the Lithium Exploration. , 2018, , .		2
44	Using Insar Stacking Techniques to Predict Bridge Collapse Due to Scour. , 2018, , .		1
45	SAR applications using TanDEM-X Alternating Bistatic data. , 2013, , .		Ο
46	Principal slope estimation at SAR building layovers. , 2014, , .		0
47	TanDEM-X DSM uncertainty measures and demonstrations. , 2015, , .		Ο
48	Comparison of the TanDEM-X response between vertical and horizontal oriented vegetation. , 2015, , .		0
49	Surface changes at the northwest Vatnajökull glacier, iceland, during the 2014–2015 Bardarbunga eruption. , 2016, , .		0
50	Interferometric SAR for characterization of wetland lakes as a function of suspending sediment cover and depth. , 2017, , .		0
51	Rice Plant Height Monitoring from Space with Bistatic Interferometry. , 2017, , .		0
52	Topographical changes caused by the 2016 central Italy earthquake series. , 2017, , .		0
53	The Novasar UK Background Mission. , 2019, , .		0